

## POLARIZATION BY ROTATIONALLY DISTORTED ELECTRON SCATTERING ATMOSPHERES

JOSEPH P. CASSINELLI AND BERNHARD M. HAISCH

Washburn Observatory, University of Wisconsin-Madison

Received 1973 September 7

### ABSTRACT

The polarization to be expected from rotationally distorted early-type stars is determined using results of calculations of the transfer of linearly polarized light in extended atmospheres. Polarization as high as about 6 percent is found for a disk envelope model and 2 percent for a Roche atmospheric model. The factors controlling the direction of the polarization are discussed. Plausible explanations are offered for the anomalous wavelength dependence of both the degree of polarization in the Wolf-Rayet star HD 50896 and of the direction of polarization in the Be star HD 45677.

*Subject headings:* atmospheres, stellar — Be stars — polarization — radiative transfer — Wolf-Rayet stars

### I. INTRODUCTION

Serkowski (1970) pointed out that the only rapidly rotating early-type stars that show measurable polarization are those that have extended atmospheres or envelopes, as evidenced by the presence of emission lines. This result is consistent with the plane-parallel model calculations of Rucinski (1969) and Collins (1970) for rotationally distorted nongray atmospheres. From their calculations, they found the polarization

in the visible to be very small, about 0.1 percent, as compared with the observed polarizations of 1-2 percent. Models of complexity comparable to those of Rucinski or Collins are not available for extended atmospheres. However, we can investigate the simpler problem of polarization by pure electron scattering atmospheres that are geometrically extended, using the numerical results of Cassinelli and Hummer (1971, hereafter CH). In that paper the transfer equation for scattering according to the Rayleigh law was solved

TABLE 1  
 COMPONENTS OF POLARIZED INTENSITY VERSUS IMPACT PARAMETER FOR SPHERICAL MODELS

$N = 2$				$N = 3$			
$\log p$	$\log I_R$	$\log I_L$	Percent	$\log p$	$\log I_R$	$\log I_L$	Percent
*	+0.6636	+0.6636	0.000	*	+0.6317	+0.6317	0.000
-1.6990	+0.6622	+0.6617	0.059	-1.6990	+0.6314	+0.6312	0.018
-1.3991	+0.6582	+0.6561	0.234	-1.4291	+0.6304	+0.6298	0.063
-1.0000	+0.5921	+0.5800	1.393	-1.0692	+0.6245	+0.6216	0.330
-0.9000	+0.5741	+0.5553	2.157	-0.9193	+0.6172	+0.6115	0.661
-0.8000	+0.5470	+0.5183	3.306	-0.7993	+0.6064	+0.5964	1.156
-0.7000	+0.5075	+0.4643	4.967	-0.7093	+0.5933	+0.5780	1.765
-0.6000	+0.4517	+0.3885	7.264	-0.6194	+0.5733	+0.5498	2.704
-0.5000	+0.3759	+0.2864	10.266	-0.4994	+0.5293	+0.4874	4.816
-0.4000	+0.2771	+0.1551	13.950	-0.4095	+0.4754	+0.4103	7.471
-0.3000	+0.1538	-0.0060	18.184	-0.3195	+0.3934	+0.2927	11.537
-0.2000	+0.0057	-0.1956	22.760	-0.1995	+0.2223	+0.0504	19.536
-0.1000	-0.1661	-0.4107	27.437	-0.1096	+0.0390	-0.2007	26.913
0.0000	-0.3596	-0.6476	31.991	+0.0104	-0.2757	-0.6124	36.928
+0.1000	-0.5723	-0.9021	36.249	+0.1003	-0.5546	-0.9608	43.631
+0.2000	-0.8014	-1.1704	40.096	+0.1903	-0.8600	-1.3285	49.249
+0.3000	-1.0444	-1.4490	43.479	+0.3103	-1.2954	-1.8325	54.998
+0.4000	-1.2988	-1.7350	46.389	+0.4148	-1.6895	-2.2663	58.108
+0.5000	-1.5625	-2.0264	48.848	+0.5171	-2.0855	-2.6973	60.712
+0.6000	-1.8337	-2.3213	50.898	+0.6194	-2.4869	-3.1241	62.523
+0.7000	-2.1110	-2.6186	52.590	+0.6961	-2.7902	-3.4413	63.497
+0.8000	-2.3930	-2.9175	53.975	+0.7984	-3.1962	-3.8611	64.424
+0.9000	-2.6789	-3.2173	55.105	+0.9006	-3.6036	-4.2778	65.050
+1.0000	-2.9678	-3.5178	56.029	1.0029	-4.0118	-4.6923	65.469
+1.1000	-3.2592	-3.8190	56.795	1.1051	-4.2033	-5.1052	65.754
+1.2000	-3.5526	-4.1210	57.456	1.2074	-4.8291	-5.5171	65.954
+1.5000	-4.4448	-5.0424	59.669	1.5142	-6.0579	-6.7563	66.629

\* The first row refers to values at the center of the disk where  $p = 0$ .

for atmospheres in which the density followed a law of the form  $r^{-N}$ ,  $N = 2$  or  $3$ . The calculations involved the solution of the transfer equation along a set of parallel rays and provided the components of the emergent intensity  $I_L$  and  $I_R$  versus the impact parameters of the rays. In the models discussed in this paper the radiation field in the distorted atmosphere comes primarily from spherically symmetric core regions. Hence the coordinate system we use to describe the components of the intensity is the same as that appropriate to a spherical model. That is, relative to the center of the star,  $I_L$  is the radial component of the intensity and  $I_R$  is the tangential component (Chandrasekhar 1950). The emergent intensity components at a wide range of impact parameters are given in table 1 along with the percent polarization of these intensities. At the limb of an extended atmosphere (i.e., at a line of sight having tangential optical depth unity) the polarization is very large, approximately 50 percent, compared with 11 percent at the limb of a plane-parallel model. This high polarization is due to the strong forward peaking of the radiation field that occurs in extended atmospheres. CH suggested that this large polarization explains the observations of Serkowski noted earlier.

However, the large polarization calculated by CH does not necessarily lead to large observed effects for two reasons. First, the apparent disk of the star must be distorted in some way for the polarization to be observable in the flux from the star. This distortion may arise from rapid rotation or from occultation. Second, while it is true that the percent polarization increases to large values toward the limb of an extended atmosphere, it is also true that the limb darkening is much more severe than in a plane-parallel atmosphere. Thus the actual contribution of the outer regions of the disk may be quite small. Therefore, specific models for the distorted shape must be considered.

## II. THE CALCULATIONS

We considered two geometrical shapes: a disk model; and one with the shape of a rigidly rotating star, a Roche model. These are shown in figure 1. In both cases we calculated the polarization as seen by a distant observer in the equatorial plane.

The disk model is a spherical model of radius  $R$  that has been truncated above a given surface latitude in both hemispheres. It is cylindrically symmetric and may be parametrized by the distance  $d$ , where  $2d$  is the thickness of the disk. The density was assumed to vary as  $r^{-N}$ ,  $N = 2$  or  $3$ , so the results of CH could be used. A similar model was used by Kitchin (1970) for analyzing emission lines from Be star envelopes. We will call the material within a distance  $d$  from the center, the "core," which is spherical in our model.

For this model we assumed that the source functions for both  $I_R$  and  $I_L$  depend only on the distance from the center, in the same way as the source functions in CH. This assumption implies that  $I_R$  and  $I_L$  at the surface are the same as those found by CH, some of which are given in table 1. Of course, the

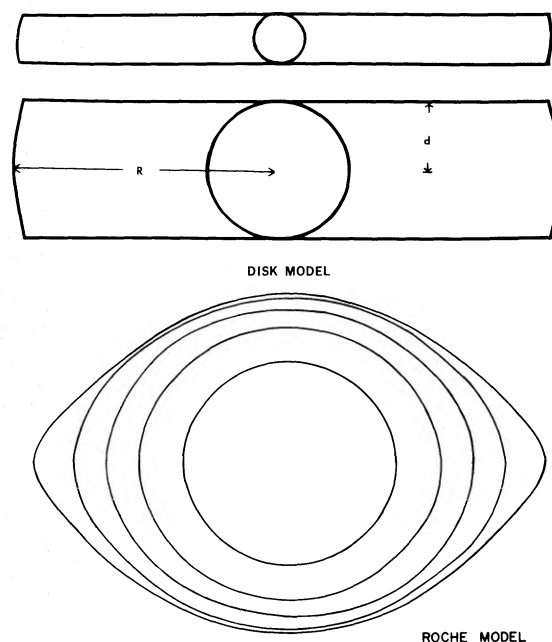


FIG. 1.—The two types of geometrical models used in the calculations. *Upper portion*, two examples of disk models with different values of the core radius  $d$ . *Lower portion*, five projected equidensity surfaces of the Roche model.

source function in the disk region is not really the same as for the spherical case since the true radiation field of the disk region would not be axisymmetric as it is in a sphere. Thus the model holds best for cases in which most of the radiation comes from the core and the disk region outside the core is optically thin. Figure 2 of CH shows that even at an optical depth as large as 2, the radiation field is rather strongly forward peaked (i.e., comes primarily from the core region) for the density laws we are considering. Therefore, as long as the regions that are truncated are regions that are optically thin in the spherically symmetric models of CH, the inclusion of their effects on the source function—which should now, of course, be identically zero—is a negligible error.

The components of the polarized intensity were integrated over the surface of the apparent disk to form the components of the polarized flux parallel and perpendicular to the polar axis. This integration is outlined by equations (3)–(6) of Harrington and Collins (1968).

The light from the undistorted core of radius  $d$  leads to no net polarization because of circular symmetry about the line of sight. As  $d$  increases, so does the fraction of the light that is unpolarized, leading to a decrease in the polarization observable in the integrated flux. The results are given in figure 2, which shows the percent polarization versus core radius  $d$  for the  $N = 2$  and  $N = 3$  density distributions. A dashed line is used for the results of models which have the core at optical depth greater than unity, measured inward along the equatorial plane. Our use of the spherical emergent intensities is

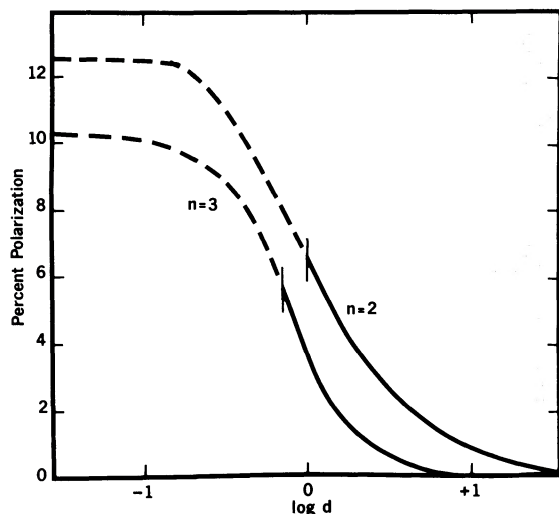


FIG. 2.—Percent polarization plotted against core radius  $d$  for the density falling off as  $1/r^2$  and  $1/r^3$ . The vertical lines indicate the polarization for the core at optical depth unity.

inaccurate for these models, for the reasons stated above.

For a model with the core at optical depth unity the polarization is 5.6 percent for a disk model with  $N = 3$  and 6.6 percent for the  $N = 2$  case.

The results for the disk model are somewhat larger than the maximum polarization observed in the rapidly rotating B star. So let us now consider a model with a more conventional extended atmospheric shape. The atmosphere is presumably extended by, say, effects of radiation pressure gradients, and is then distorted by rapid rotation. The polar radius of a rigidly rotating star (i.e., a Roche model) whose equator is rotating at the critical speed is two-thirds the equatorial radius. Deeper in the atmosphere the isodensity surfaces are less distorted, and at a polar radial distance of 0.4 times the polar radius the surface is distorted by less than 1 percent. In analogy to the previous model we refer to this as the “undistorted core.” The density is arbitrarily assumed to fall as  $r^{-3}$  along the polar axis, and the Roche cubic equation (cf. Harrington and Collins 1968) is solved to find the isodensity surfaces at any given polar angle. The radius scale for the density distribution is arbitrary, so we can freely choose the core to be at some given optical depth along the pole. We ignore that part of the  $r^{-3}$  density distribution that lies beyond the critical surface.

To evaluate the net polarization, we integrate the transfer equation along many lines of sight through the disk of the star and then, as before, integrate the emergent intensities over the distorted disk area. The source functions for linear polarization involve the moments  $J_L$ ,  $K_L$ , and  $J_R$  (Chandrasekhar 1950), and these were evaluated in CH for the spherical problems.

For the intensity integration, we used the Feautrier scheme and approximated the source function along these rays in several different ways. First we simply used the source function from the spherical models,

along the polar axis and assumed that the isodensity surfaces were also surfaces of constant source function. Second we modified the source function along the isodensity surfaces in proportion to the increase in radial distance, at some given polar angle, over the polar distance to that surface. The mean intensities appearing in the source function,  $J_R$ ,  $J_L$ , and  $K_L$ , were modified by an amount depending on the angle  $\theta_c$  subtended by the core. Thus the moment  $J$  was varied proportional to  $1 - \mu_c$  and  $K$  to  $1 - \mu_c^3$ , where  $\mu_c = \cos \theta_c$  (cf. Lucy 1970). The last source-function distribution was determined by iteration. A calculation using the spherical source function, i.e., the first case mentioned above, was used to provide intensities at various positions in the atmosphere. These were integrated over angle, in a method analogous to that discussed in Hummer and Rybicki (1971), to provide revised intensity moments which in turn were used in a second set of ray integrations.

The maximum polarization occurred with the core at about optical depth 2, and polarizations of 2.3, 1.3, and 1.6 percent were found for the spherical, cone-approximation, and iterative source functions, respectively.

These polarizations are within the observed range of polarizations as summarized by Serkowski (1970). If the history of the plane-parallel calculations may be used as a guide (cf. Collins 1970), we should expect that the inclusion of absorptive opacity will decrease the theoretical polarizations in the visual significantly. We must remember, however, that the density at any given optical depth will be several orders of magnitude smaller in an extended atmosphere than in the plane-parallel atmosphere, as is familiar from the comparison of supergiant and main sequence atmospheres. Code (1951) found that the polarization of the intensity at the limb of a star decreases somewhat faster than  $(1 - \lambda)$ , where  $\lambda$  is the ratio of absorptive to total opacity, [ $\lambda = \kappa/(\kappa + \sigma)$ ]. For the electron density and temperature at optical depth  $\frac{2}{3}$  in a main-sequence star with effective temperature 20,000° K,  $\lambda$  is 0.97 at 5000 Å. Thus absorptive opacity dominates, and the polarization is quenched as in Collins's (1970) models. For an electron density three orders of magnitude smaller, as is appropriate for an extended atmosphere, the ratio is 0.03. Hence, scattering is the dominant form of opacity; and since the required anisotropy of the radiation field is due to geometrical effects, we should expect observable polarization in the visible. Nevertheless, the very largest polarizations observed in B stars (i.e., those larger than 1.5 percent) can probably be explained only by the disk envelope model.

In all of our models the direction of the net polarization is parallel to the polar axis. This is opposite (i.e., the position angle is different by 90°) to that found by Harrington and Collins (1968) and Collins (1970). In our investigation into the cause of this difference it has become clear that the direction of polarization depends on a rather delicate balance of several effects.

As was noted earlier, the contribution of any unit surface area to the net polarization depends on two

factors: the magnitude of the emergent intensity, and the degree of polarization of that intensity. The magnitude of the intensity depends on  $\int S e^{-\tau} d\tau$ , where  $S$  is the source function. For integration rays which are optically thick, which is the case for any ray in the plane-parallel approximation, the intensity is roughly equal to the source function at optical depth unity. The pole (or "gravity") brightening in a rotating plane parallel star is a pertinent example of a case in which the magnitude of the intensity weights one region of the atmosphere over other regions. It tends to lead to a net polarization that is perpendicular to the polar axis. For integration rays that are optically thin, as occurs near the limb of an extended atmosphere the emergent intensity does not tend toward any particular value of the source function but to a product  $S\tau$ . Thus in a rotationally distorted star a line of sight near the limb, which grazes some isodensity surface at its point of closest approach to the center, will have an optical depth larger than a line of sight grazing the same surface at the pole, simply because the surfaces of equal density are separated by a larger geometrical distance. Thus, as  $\tau$  is larger, "equatorial brightening" is possible. This brightening of the equatorial extremities relative to the polar regions indeed occurs for some of our models and presumably in every case reduces the polar brightening. This effect, along with the obvious fact that there is larger surface area at the extreme equatorial regions, tends to lead to a polarization directed parallel to the polar axis.

The net direction of polarization of the model depends also on the *degree* of polarization of radiation from various areas of the disk. This is controlled by the amount of forward peaking of the radiation field (Code 1950; Harrington 1970; Collins 1970; Cassinelli and Hummer 1971). For extended electron scattering atmospheres, the forward peaking is simply a geometrical effect. For plane-parallel atmospheres, the forward peaking near the limb can arise because of a steep source-function gradient. The source-function gradient depends on wavelength in a nongray atmosphere, and in a distorted atmosphere it also depends on position along the limb. At the pole of a Roche model, the temperature gradient and so the gradient of the integrated Planck function,  $dB/d\tau$ , is steeper than at the equator. This is because the isodensity surfaces are also surfaces of equal pressure and hence of equal temperature. The wavelength dependence arises because of the behavior of the Planck function at different frequencies. In the ultraviolet (i.e., in the Wien's approximation region)  $dB_v/d\tau \gg dB/d\tau$ , whereas in the visual (i.e., Rayleigh-Jeans region)  $dB_v/d\tau \approx dB/d\tau$ . This causes the radiation field at the surface to be more anisotropic, peaked

more strongly in the forward direction, in the ultraviolet, and consequently the light scattered from the outermost layers is more highly polarized than in the visual. These factors lead to a larger polarization at the pole than at the equator and to a greater difference in the ultraviolet than in the visual.

In Collins's models the net polarization is always perpendicular to the polar axis and is larger in the ultraviolet than in the visual, primarily because of the effect of the source-function gradient and the polar brightening. In our extended electron-scattering models the effects of increased surface area, increased forward peaking of the field at the equatorial regions, and perhaps equatorial brightening lead to the direction of the net polarization being parallel to the polar axis.

If we were to have absorptive opacity in our models, we would make the effect of the source-function gradient more important than in our present models. Thus we should expect that there should be a wavelength dependence of the direction of the polarization. The direction would be parallel to the axis at wavelengths where area effects, geometrical peaking, and equatorial brightening can dominate the source-function gradient and polar brightening, and perpendicular at wavelengths where the reverse situation holds. It is interesting to note that Zellner and Serkowski (1972) have reported observations by Coyne of the Be star HD 45677 in which the direction of polarization changes sign with wavelength. (They suggest that the effect could be due to solid dielectric grains.)

The mechanism we discuss above for rotation of the polarization plane can also be used to explain the observation of the Wolf-Rayet star HD 50896 in which the polarization is larger in the visual than in the ultraviolet (Serkowski 1970; Zellner and Serkowski 1972). This is certainly not expected on the basis of Collins's results because the factors influencing polarization are always greater in the ultraviolet. However, if the polarization in the visual is aligned parallel to the polar axis, it can decrease as the effect of the source-function gradient becomes more important. The net result will be not a change of direction of the polarization, but just a decrease. It is quite apparent from these examples that the intrinsic polarization of stars is a potentially powerful diagnostic tool to determine the structure of stellar atmospheres.

We wish to thank George W. Collins II for suggesting the problem and for several helpful discussions, and John S. Mathis for his suggestions and for his advice concerning the Roche model. This research was partially supported by the National Science Foundation.

#### REFERENCES

- Cassinelli, J. P., and Hummer, D. G. 1971, *M.N.R.A.S.*, **153**, 9 [CH].  
 Chandrasekhar, S. 1950, *Radiative Transfer* (Oxford: Oxford University Press).  
 Code, A. D. 1950, *Ap. J.*, **112**, 22.  
 Collins, G. W., II. 1970, *Ap. J.*, **159**, 583.  
 Harrington, J. P. 1970, *Astr. and Space Sci.*, **8**, 227.  
 Harrington, J. P., and Collins, G. W., II. 1968, *Ap. J.*, **151**, 1051.  
 Hummer, D. G., and Rybicki, G. B. 1971, *M.N.R.A.S.*, **152**, 1.  
 Kitchin, C. R. 1970, *M.N.R.A.S.*, **150**, 455.  
 Lucy, L. B. 1970, *Ap. J.*, **193**, 95.  
 Rucinski, S. M. 1970, *Acta Astr.*, **20**, 1.  
 Serkowski, K. 1970, *Ap. J.*, **160**, 1083.  
 Zellner, B. H., and Serkowski, K. 1972, *Pub. A.S.P.*, **84**, 619.